



Original Article



# Exosome-transported circHDAC1\_004 Promotes Proliferation, Migration, and Angiogenesis of Hepatocellular Carcinoma by the miR-361-3p/NACC1 Axis

Bin Xu<sup>1,2,3,4#</sup>, Wenbo Jia<sup>1,2,3,4#</sup>, Yanzhi Feng<sup>1,2,3,4</sup>, Jinyi Wang<sup>1,2,3,4</sup>, Jing Wang<sup>5</sup>, Deming Zhu<sup>1,2,3,4</sup>, Chao Xu<sup>1,2,3,4</sup>, Litao Liang<sup>1,2,3,4</sup>, Wenzhou Ding<sup>1,2,3,4</sup>, Yongping Zhou<sup>6\*</sup> and Lianbao Kong<sup>1,2,3,4\*</sup>

<sup>1</sup>Hepatobiliary Center, The First Affiliated Hospital of Nanjing Medical University, Nanjing, Jiangsu, China; <sup>2</sup>Key Laboratory of Liver Transplantation, Chinese Academy of Medical Sciences, National Health Commission Key Laboratory of Living Donor Liver Transplantation (Nanjing Medical University), Nanjing, Jiangsu, China; <sup>3</sup>Jiangsu Provincial Medical Innovation Center, Nanjing, Jiangsu, China; <sup>4</sup>Jiangsu Provincial Medical Key Laboratory, Nanjing, Jiangsu, China; <sup>5</sup>Department of health, Affiliated Hospital of Stomatology, Nanjing Medical University, Nanjing, Jiangsu, China; <sup>6</sup>Jiangnan University Medical Center, JUMC, Department of Hepatobiliary, Wuxi, Jiangsu, China

Received: 10 November 2022 | Revised: 26 January 2023 | Accepted: 15 February 2023 | Published online: 22 March 2023

## Abstract

**Background and Aims:** Hepatocellular carcinoma (HCC) is among the most common malignant tumors globally. Circular RNAs (circRNAs), as a type of noncoding RNAs, reportedly participate in various tumor biological processes. However, the role of circHDAC1\_004 in HCC remains unclear. Thus, we aimed to explore the role and the underlying mechanisms of circHDAC1\_004 in the development and progression of HCC. **Methods:** Quantitative real-time polymerase chain reaction (qRT-PCR) was used to detect circHDAC1\_004 expression (circ\_0005339) in HCC. Sanger sequencing and agarose gel electrophoresis were used to determine the structure of circHDAC1\_004. *In vitro* and *in vivo* experiments were used to determine the biological function of circHDAC1\_004 in HCC. Herein, qRT-PCR, RNA immunoprecipitation, western blotting, and a luciferase reporter assay were used to explore the relationships among circHDAC1\_004, miR-361-3p, and NACC1. **Results:** circHDAC1\_004 was upregulated in HCC and significantly associated with poor overall survival. circHDAC1\_004 promoted HCC cell proliferation, stemness, migration, and invasion. In addition, circHDAC1\_004 upregulated human umbilical vein endothelial cells (HUVECs) and promoted angiogenesis through exosomes. circHDAC1\_004

promoted NACC1 expression and stimulated the epithelial-mesenchymal transition pathway by sponging miR-361-3p. **Conclusions:** We found that circHDAC1\_004 overexpression enhanced the proliferation, stemness, and metastasis of HCC via the miR-361-3p/NACC1 axis and promoted HCC angiogenesis through exosomes. Our findings may help develop a possible therapeutic strategy for HCC.

**Citation of this article:** Xu B, Jia W, Feng Y, Wang J, Wang J, Zhu D, *et al.* Exosome-transported circHDAC1\_004 Promotes Proliferation, Migration, and Angiogenesis of Hepatocellular Carcinoma by the miR-361-3p/NACC1 Axis. J Clin Transl Hepatol 2023. doi: 10.14218/JCTH.2022.00097.

## Introduction

Primary liver cancer is the second most common malignant tumor worldwide, and hepatocellular carcinoma (HCC) is its most common pathological type.<sup>1</sup> Because of the high rate of hepatitis B virus infection, China accounts for nearly half of newly diagnosed HCC cases and HCC-related deaths worldwide.<sup>2</sup> Although several treatments, such as surgical resection, liver transplantation, chemotherapy, radiation therapy, immunotherapy, and molecular targeted therapy, have shown survival benefit, the prognosis of HCC remains poor, particularly due to challenges with early diagnosis and the recurrence and metastasis of HCC cells.<sup>3</sup> Therefore, there is an urgent need to understand the mechanisms of HCC and develop new treatment strategies.

Circular RNAs (circRNAs) are a class of noncoding RNAs (ncRNAs) that feature a reverse splicing closed loop. circRNAs mediate multiple biological functions, and they are reportedly involved in tumorigenesis and development.<sup>4</sup> circRNAs can act as endogenous competitive inhibitors by sponging miRNAs and interacting with RNA-binding proteins to regulate transcription.<sup>5</sup> However, their role in HCC and their specific molecular mechanisms warrant further investigation.

HDAC1, a member of the histone deacetylase (HDAC)

**Keywords:** circHDAC1\_004; Exosome; Angiogenesis; Hepatocellular carcinoma; Stemness; Epithelial-mesenchymal transformation.

**Abbreviations:** CCK8, cell counting kit 8; ceRNA, competing endogenous RNA; circRNA, circular RNA; EdU, 5-Ethynyl-20-deoxyuridine; FISH, fluorescence in situ hybridization; HCC, hepatocellular carcinoma; HDAC1, Histone deacetylase 1; HUVECs, human umbilical vein endothelial cells; miRNAs, microRNAs; NACC1, Nucleus Accumbens Associated 1; NC, negative control; ncRNA, noncoding RNA; PBS, phosphate buffered saline; qRT-PCR, quantitative real-time polymerase chain reaction; RIP, RNA binding protein Immunoprecipitation; siRNA, small interfering RNA.

\*Contributed equally to this work.

**\*Correspondence to:** Lianbao Kong, Hepatobiliary Center, The First Affiliated Hospital of Nanjing Medical University, 300 Guangzhou Road, Nanjing, Jiangsu 210029, China. ORCID: <https://orcid.org/0000-0003-2508-1321>. Tel: +86-13 801583199, Fax: +86-25-68303221, E-mail: lbkong@njmu.edu.cn; Yongping Zhou, Department of Hepatobiliary Surgery, Jiangnan University Medical Center, JUMC, No. 68 Zhongshan Road, Wuxi, Jiangsu 214000, China. Tel: +86-15052115599, Fax: +86-510-68562571, E-mail: zyp19840527@njmu.edu.cn

family, mediates epigenetic regulation, which plays an important role in normal development and tumor progression.<sup>6</sup> Presently, there is ample literature supporting the promotion effect of HDAC1 in HCC. In cancer cells, HDAC1 inhibits the tumor suppressor genes p21WAF1/CIP1 and Bax, resulting in abnormal cell proliferation and cell viability.<sup>7,8</sup> The impact of HDAC1 on HCC progression has been widely acknowledged. For example, HDAC1 knockdown reduces cyclin-dependent kinase (CDK) levels and inhibits HCC cell proliferation.<sup>9</sup> HDAC1 regulates HCC in complex and diverse ways, and these distinct mechanisms require further investigation. Through database analysis, we found that HDAC1 transcribed circRNAs. The function of HDAC1-derived circRNAs in HCC has not yet been investigated.

Exosomes are small nanoscale vesicles that transport bioactive molecules between cells and regulate the intercellular microenvironment and immune system.<sup>10</sup> Studies have shown that exosomes, as mediators of cell-to-cell communication, are involved in tumor development, metastasis, immune evasion, and drug resistance.<sup>11</sup> An increasing number of studies have shown that circRNAs in exosomes are abundant and stable, but the function of circRNAs in exosomes remains unclear.

In this study, we showed that circHDAC1\_004 expression was higher in HCC than in paraneoplastic tissues. The increased expression promoted HCC proliferation, metastasis, and stemness through the miR-361-3p/NACC1 axis. In addition, circHDAC1\_004 could be transferred from HCC cells to human umbilical vein endothelial cells (HUVECs) by exosomes to promote HCC angiogenesis.

## Methods

### HCC samples

The HCC and paracancerous tissues used in this study were obtained from the Hepatobiliary Center of the First Affiliated Hospital of Nanjing Medical University. All human tissue samples were obtained with patients' written consent. This study was approved by the Ethics Committee of the First Affiliated Hospital of Nanjing Medical University.

### Cell lines

HCC cell lines Huh7, MHCC97H, HepG2, Hep3B, MHCCLM3, SK-Hep1, YY8103, a normal human liver cell line (HHL-5), and HUVECs were purchased from the Shanghai Institute of Cell Biology, Chinese Academy of Sciences (Shanghai, China). All cell lines were cultured in Dulbecco's Modified Eagle Medium (DMEM; Gibco, Carlsbad, CA, USA) medium with 10% fetal bovine serum (Gibco), 50 U/mL penicillin (Invitrogen, Waltham, MA, USA), and 50 U/mL streptomycin (Invitrogen). All cells were cultured in a 5% CO<sub>2</sub> incubator at 37°C.

### Quantitative real-time polymerase chain reaction (qRT-PCR)

RNA was extracted from cells or tissues using TRIzol reagent (Invitrogen). RNA concentration was measured using a spectrophotometer. For qRT-PCR detection of circular and mRNA, the RNA was reverse-transcribed to cDNA using a reverse transcription kit (VA zyme, Nanjing, China). qRT-PCR was performed using Ace qPCR SYBR Green Master Mix (VA zyme) with an ABI 7900 PCR system (Applied Biosystems Inc., Waltham, MA, USA), and GAPDH was used as the negative control.

For qRT-PCR detection of miRNA, miDETECT A Track miRNA qRT-PCR primer (Ribobio, Guangzhou, China) and miDETECT A Track miRNA qRT-PCR Starter Kits (Ribobio) were

used. In brief, total RNA was added with ploy(A) tailing and then reverse-transcribed to cDNA. Specific qRT-PCR was performed with miDETECT A Track miR-361-3p and miR-194-5p qPCR primer and miDETECT A Track Uni-Reverse Primer. U6 was used as the negative control. Primers used in this study are enlisted in the Supplemental Material (Supplementary Table 1).

### Agarose gel electrophoresis

Divergent and convergent primers (Ribobio) of circHDAC1\_004 were used to amplify cDNA and gDNA of HCC cell lines, respectively, and the amplified products were collected. A 1× Tris-acetate-EDTA buffer (Beyotime, Nantong, China) solution was used to prepare 1% agarose gels that were boiled and cooled and nucleic acid stain was added. The above products were added into the agarose gel, and 1× TAE was used as the electrophoresis solution, which was performed at 100 V for 1 h, and the position of the bands was observed under ultraviolet lamp.

### Cell proliferation, migration, and invasion assays

Cell proliferation, migration, and invasion assays were performed as described in the Supplementary Methods (Supplementary File 1).

### Fluorescence in situ hybridization (FISH)

FISH was performed with a commercially available kit (Ribobio). The appropriate number of cells was added to each well of a 24-well plate. After the cells were fixed with 4% paraformaldehyde, the cell membrane was disrupted with 0.5% Triton X-100. Cells were blocked with prehybridization solution, and 100 µL of hybridization solution containing circHDAC1\_004 FISH probe, 18S probe, and U6 probe (Ribobio) was added to each well and was protected from the light. The cells were hybridized overnight at 37°C and counterstained for 10 min with 4',6-diamidino-2-phenylindole (DAPI). Images were taken with a confocal laser microscope (Stellaris STED; Leica, Frankfurt, Germany).

### Sphere formation

Experimental cells (2,000 cells/well) were seeded into low adhesion 6-well plates. Herein, 2 mL of stem cell medium [DMEM/F12 (Gibco) supplemented with 1XB27 (Invitrogen), 20-ng/mL FGF (Gibco), 20-ng/mL EGF (Gibco), and 4-µg/mL heparin (Selleck, Houston, TX, USA)] was added to each well, and the cells were cultured for 10 days at 37°C in an incubator containing 5% CO<sub>2</sub>. The state of cell pelleting was observed, and the number of pelleted cells was calculated.

### Immunofluorescence

A slide was placed at the bottom of the 24-well plate, and 40,000 treated cells were added to each well. When the cells had attached to the plate surface, they were fixed in paraformaldehyde, lysed with Triton, and blocked with goat serum for 30 min. The cells were incubated with primary antibody overnight. After incubation with a fluorescent secondary antibody (Beyotime) for 1 h, the nuclei were labeled with DAPI (Beyotime). Images were taken using a confocal microscope.

### Xenograft nude mouse model

All animal experiments in this study were approved by the Institutional Animal Care and Use Committee (IACUC) of the First Affiliated Hospital of Nanjing Medical University. All animal-related operations were performed according to the IACUC operating guidelines. Four-week-old male BLAB/C

Xu B. *et al*: circHDAC1\_004 promotes HCC progression.

nude mice (Vital River, Beijing, China) were divided into four groups, with six mice in each group. Then, 5 million lentivirus-transfected cells were injected into the axilla of the left upper limb of each mouse. Subcutaneous tumor volume was recorded every 3 days for 30 days, and then the mice were euthanized. Subcutaneous tumors were removed for immunohistochemistry and volume measurements.

#### **Pulmonary metastasis model**

Four-week-old male BLAB/C nude mice (Vital River) were divided into four groups, with six mice in each group. Then, 1.5 million experimental cells were injected into the mice via the tail vein. Six weeks later, the mice were euthanized and their lungs were collected for photography and hematoxylin and eosin (HE) staining.

#### **Exosome extraction**

Exosomes were extracted by gradient centrifugation. Briefly, the cell supernatant was placed in a clean centrifuge tube (Beckman, Brea, CA, USA) and centrifuged at 500 *g* for 10 min, 2,000 *g* for 20 min, and 10,000 *g* for 30 min. After each centrifugation, the supernatant was removed and placed in a clean Beckman tube. Samples were then centrifuged twice at 110,000 *g* for 1 h. The precipitated exosomes were resuspended in phosphate-buffered saline.

#### **Exosome identification**

Extracted exosomes were imaged and verified by a projection electron microscope (JEM-1010; JEM, JEOL, Japan) at the Analysis and Testing Center of Nanjing Medical University. The particle size distribution range of exosomes was examined by particle point titration and using a particle size analyzer to judge the purity and concentration of the extracted exosomes. Proteins were extracted from these exosomes, and the exosome-related proteins CD81, CD9, and TSG101 were detected by western blotting.

#### **Exosome uptake**

A total of 1 mL of preprepared working solution PKH67 (PKH67: diluent=1:250; War bio, Nanjing, China) was added to the exosome suspension. Samples were incubated for 3 min at room temperature. Then, exosomes were precipitated by centrifugation at 110,000 *g* for 70 min. Exosomes were suspended and incubated with cells for 12 h. After fixation with paraformaldehyde, nuclei were labeled with DAPI and imaged under a laser confocal microscope (LSM5 Live; Zeiss, Oberkochen, Germany).

#### **Tubule formation**

Fifty microliters of Matrigel matrix (BD Biosciences, Franklin Lakes, NJ, USA) was added to each well of a 96-well plate, and the plate was placed in the incubator at 37°C until the Matrigel matrix solidified on the plate. HUVECs were resuspended at 40,000/mL in exosome-free medium, and 50  $\mu$ M of the cell suspension was added to each well. After 8 h, tubules of HUVEC cells were observed by light microscopy, and the experimental results were photographed.

#### **RNA immunoprecipitation (RIP)**

Cell lysates were incubated overnight with magnetic beads (Genesee, Guangzhou, China) coupled with the Ago2 antibody or IgG at 4°C. Then, the beads were washed and incubated with protease K to remove proteins. Finally, RNA was extracted, and qRT-PCR was performed to determine whether circHDAC1\_004 and miR-361-3p had bind with Ago2.

#### **Pull-down assay**

A biotin-labeled circHDAC1\_004 probe and its negative control sequence were synthesized *in vitro*. The RNA-RNA complex was captured using a Pierce magnetic RNA-protein pull-down kit (Thermo Fisher Scientific, Waltham, MA, USA). HCC cell lines overexpressing circHDAC1\_004 were lysed and the supernatant was extracted, and DNase was added to digest the DNA. The circHDAC1\_004 probe and NC probe were added to the two supernatants for hybridization, and magnetic beads were collected using a magnetic frame. RNA on the magnetic beads was eluted, and purified RNA was reverse-transcribed into cDNA; the data were analyzed after qRT-PCR.

#### **Dual-luciferase reporter assay**

The binding site of circHDAC1\_004 with miR-361-3p were predicted using Mir DIP, and the binding site of miR-361-3p with NACC1 3' UTR was predicted by Targets can. Then, wild-type (WT) and mutant plasmids (MUT) were designed. The WT or mutant vectors were cotransfected into HEK-293T cells with miRNA mimics using transfection reagents. Then, 5 ng of sea kidney luciferase vector was added and incubated for 2 h, followed by the addition of 150  $\mu$ M of passivation lysate (PLY) to Petri dishes and incubated for 20 min on ice. Luciferase activity was measured and quantified using a dual-luciferase reporter gene assay system.

#### **Western blotting**

Cells were lysed with a radio-immunoprecipitation assay (Beyotime). Sodium dodecyl sulfate-polyacrylamide gel electrophoresis was used to isolate and transfer proteins to a polyvinylidene fluoride membrane (Merck Millipore, Burlington, MA, USA). The samples were blocked with 5% skim milk powder for 2 h and incubated in the primary antibody overnight. After washing with Tris-buffered saline and Tween20 (TBST) three times, the secondary antibody was added and the membranes were incubated for 2 h at room temperature. Protein content was quantified using a hypersensitive enhanced chemiluminescence (ECL) exposure solution and Image Lab software (Bio-Rad, Hercules, CA, USA). The primary antibodies used were GAPDH (Proteintech, Wuhan, China), CD9 (Proteintech), CD81 (Invitrogen), TSG101 (Invitrogen), E-cadherin (Proteintech), N-cadherin (Proteintech), Vimentin (Service bio), and NACC1 (Proteintech).

#### **Statistical analysis**

The results were reported as means  $\pm$  SD, and  $p < 0.05$  was considered significant. The statistical analysis was performed with GraphPad Prism v8.0 (GraphPad, San Diego, CA, USA). Experiments with multiple comparisons were compared between two groups using one-way analysis of variance. Normally distributed parameters were tested with the unpaired Student's *t*-test, and non-normally distributed parameters were tested with the Mann-Whitney test. Correlations were tested using the Spearman's correlation. Survival curves were drawn by the Kaplan-Meier method.

## **Results**

### **circHDAC1\_004 was upregulated in HCC and negatively correlated with the prognosis of HCC patients**

HDAC1 is reported to be an important oncogene in HCC. It promotes cell proliferation and regulates the cell cycle of HCC.<sup>14</sup> To further investigate the role of HDAC1-derived circRNAs in HCC, primers for 14 HDAC1-derived circRNAs were designed. Preliminary screening of HDAC1-derived circRNAs

**Table 1. Relationship between circHDAC1\_004 expression level in HCC tissues and clinical parameters of patients**

Clinicopathologic feature	Total	CircHDAC1_004		p value
	80	High (40)	Low (40)	
Age				
>60	48	21	27	0.2537
≤60	32	19	13	
Sex				
Male	40	21	19	0.8233
Female	40	19	21	
HBsAg				
Negative	15	8	7	0.9999
Positive	65	32	33	
AFP				
≤200	18	11	7	0.4225
>200	62	29	33	
Tumor number				
Single	52	19	33	0.0020
Multiple	28	21	7	
Tumor size in cm				
≤5	46	15	31	0.0006
>5	34	25	9	
TNM stage				
I	47	18	29	0.0225
II-III	33	22	11	
Microvascular invasion				
Yes	28	19	9	0.0340
No	52	21	31	
Edmondson stage				
I-II	50	18	32	
III-IV	30	22	8	

AFP, alpha fetoprotein; HBsAg, hepatitis B surface antigen.

in five pairs of HCC and paracancerous tissues by qRT-PCR revealed that five circRNAs (circHDAC1\_002, circHDAC1\_004, circHDAC1\_008, circHDAC1\_012, and circHDAC1\_014) were upregulated in HCC (Fig. 1A). We assessed the expression of the circRNAs in 80 pairs of HCC and paraneoplastic tissues, and circHDAC1\_004 expression was found to be significantly upregulated (Fig. 1B–F). Clinicopathological analysis revealed that circHDAC1\_004 expression was positively correlated with tumor volume, the TNM stage, and microvascular invasion in HCC patients (Table 1). As circHDAC1\_004 showed the most significant difference, its transcription was confirmed in the validation set (Fig. 1G). Meanwhile, Kaplan-Meier survival analysis showed that patients with higher levels of circHDAC1\_004 had shorter overall survival (Fig. 1H).

Notably, circHDAC1\_004, also known as circ\_0005339, is derived from exons 5–6 of the HDAC1 gene (Fig. 2A). Sanger sequencing was performed to check for head-to-tail splicing of circHDAC1\_004 (Fig. 2B). We also designed divergent and convergent primers to verify the circular structure of circHDAC1\_004. Agarose gel electrophoresis showed

that circHDAC1\_004 amplified by convergent primers could be detected in both cDNA and gDNA, but circHDAC1\_004 amplified by divergent primers was only detected in cDNA (Fig. 2C). Furthermore, the RNase R treatment indicated that circHDAC1\_004 was more resistant to RNase R digestion than linear RNA (Fig. 2D). To confirm the distribution of circHDAC1\_004, nucleoplasm separation experiments and FISH were performed. circHDAC1\_004 was primarily expressed in the cytoplasm (Fig. 2E, F).

#### ***circHDAC1\_004 promoted proliferation, migration, schizogenesis, and the EMT pathway of HCC cells***

To further explore the function of circHDAC1\_004 in HCC development, we downregulated circHDAC1\_004 in SK-Hep1 cells and upregulated circHDAC1\_004 in YY8103 cells by lentiviral transfection, as SK-Hep1 had the highest and YY8103 had the lowest circHDAC1\_004 expression of the tested HCC cell lines (Fig. 3A, B), and the sequence of siRNA is shown in Supplementary Table 2. The results of CCK-8, colony formation, and EdU assays indicated that circHDAC1\_004 inac-



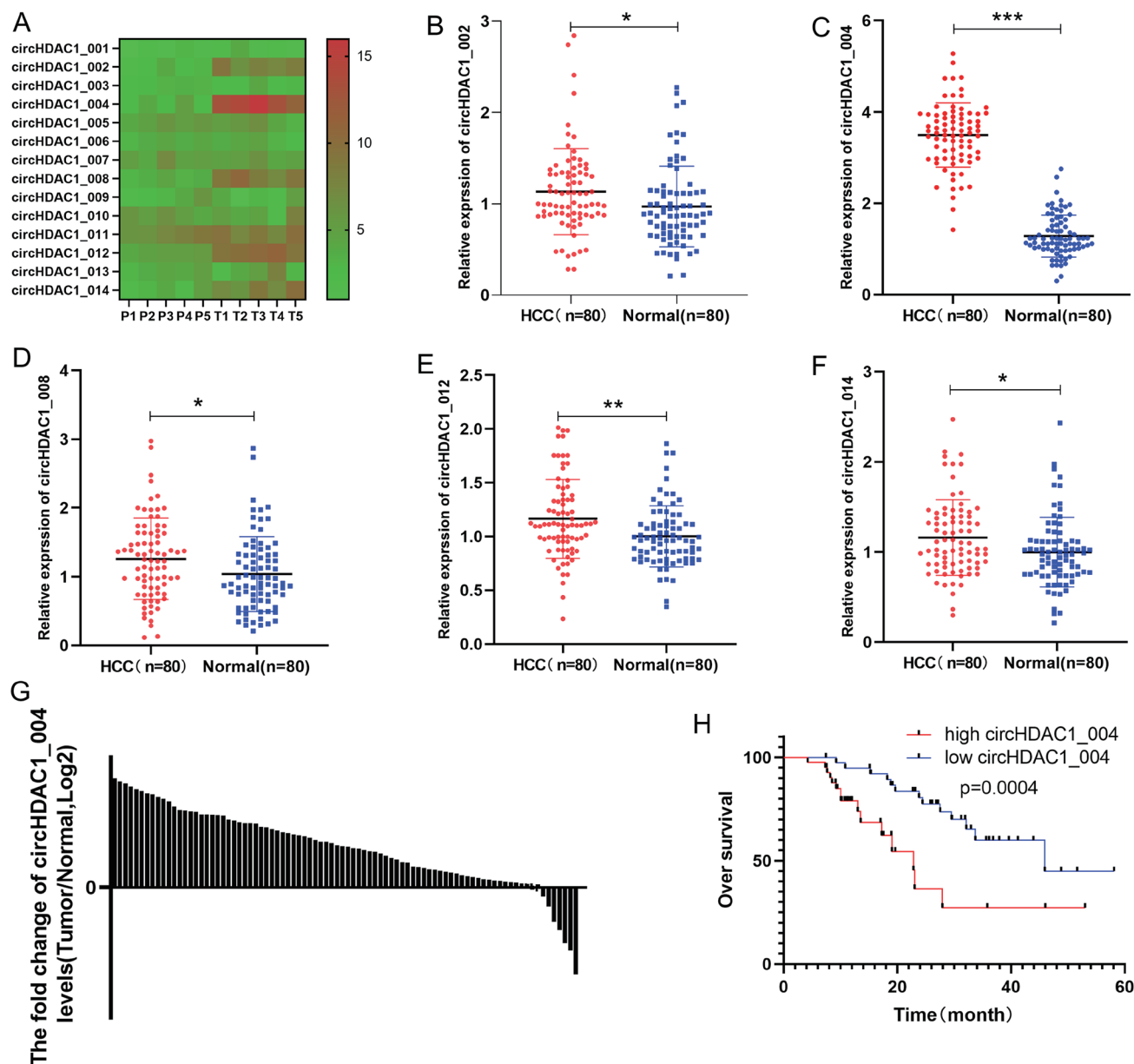


**Fig. 1. circHDAC1\_004 expression was upregulated in HCC and was associated with poor outcomes.** (A) Expression of 14 HDAC1-derived circRNAs in five pairs of HCC and paracancerous tissues was detected by qRT-PCR. (B–F) Expression of five circRNAs transcribed from HDAC1 in 80 pairs of HCC and paracancerous tissues was detected by qRT-PCR. (G) Fold-change of circHDAC1\_004 expression between HCC and paracancerous tissues. (H) Survival curve of HCC patients with circHDAC1\_004 low or high expression. Data are means  $\pm$  SD. (\* $p < 0.05$ ; \*\* $p < 0.01$ ; \*\*\* $p < 0.001$ ). circRNA, circular RNA; qRT-PCR, Quantitative real-time polymerase chain reaction.

tivation suppressed the proliferation of SK-Hep1 cells, and circHDAC1\_004 overexpression enhanced the proliferation of YY8103 cells (Fig. 3C–E). Transwell and wound healing assays showed that circHDAC1\_004 inactivation suppressed the migration and invasion of SK-Hep1 cells, whereas circHDAC1\_004 overexpression had the opposite effects (Fig. 3F, G). Moreover, a stem-cell pelleting assay showed that circHDAC1\_004 inactivation inhibited the spherogenesis ability of SK-Hep1 cells and that upregulated circHDAC1\_004 expression promoted YY8103 cell pelleting (Fig. 3H).

Epithelial-mesenchymal transformation (EMT) is a morphogenetic process associated with tumor aggressiveness, metastasis, and chemical resistance to malignancies.<sup>12</sup> West-

ern blotting (Fig. 3I) and immunofluorescence (Supplementary Fig. 1A) showed that the abundance of E-cadherin was significantly increased by circHDAC1\_004 knockdown and decreased by circHDAC1\_004 overexpression; meanwhile, the expression of N-cadherin and vimentin was significantly decreased by circHDAC1\_004 knockdown and increased by circHDAC1\_004 overexpression. The results suggest that circHDAC1\_004 promoted the EMT pathway in HCC.

#### **circHDAC1\_004 promoted HCC cell proliferation, angiogenesis, and metastasis in vivo**

We investigated the effect of circHDAC1\_004 *in vivo* by constructing a subcutaneous tumor model and nude mouse lung

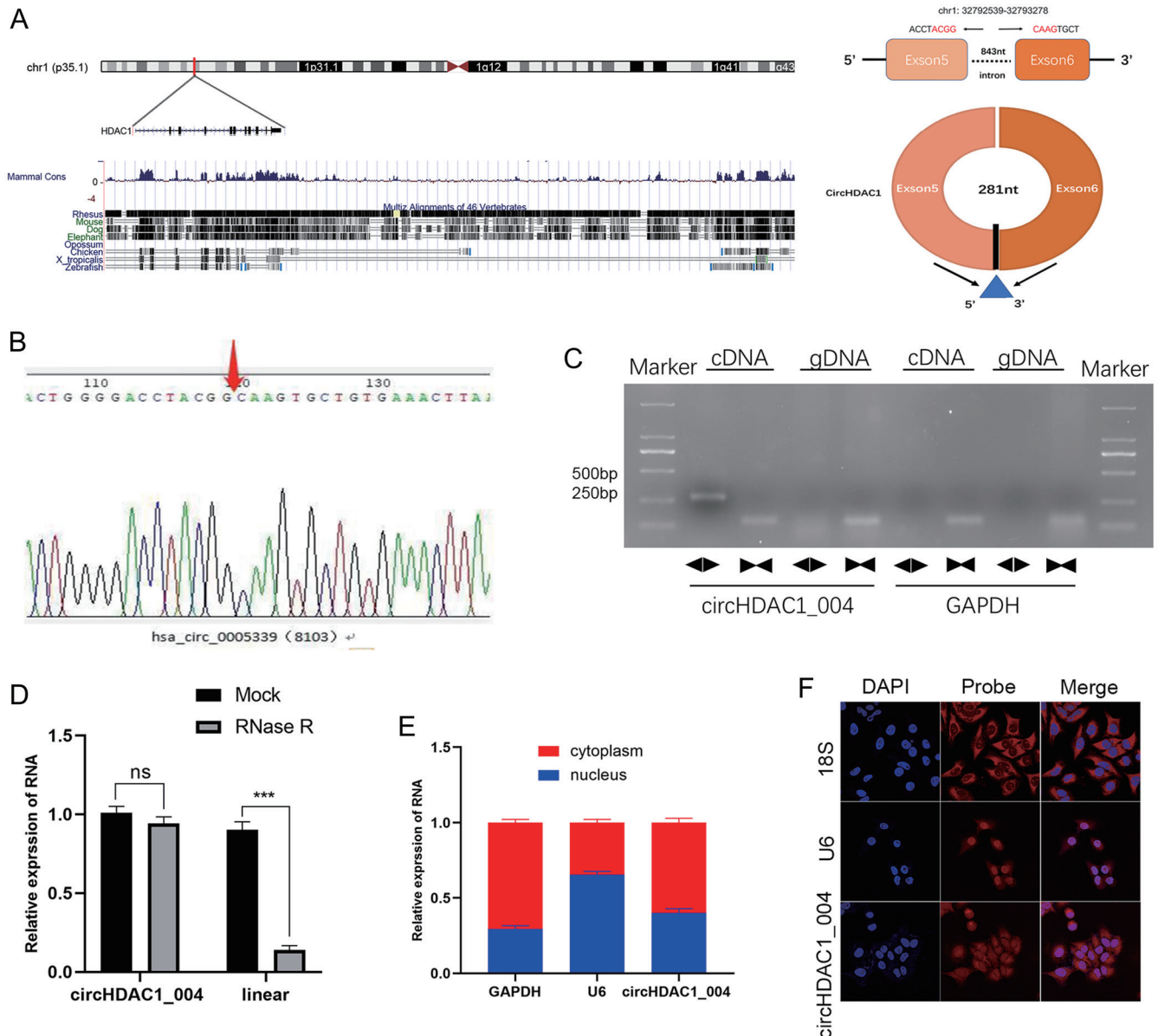


**Fig. 2. Confirmation of the circular structure of circHDAC1\_004.** (A) Schematic of the genomic location of circHDAC1\_004. (B) Sanger sequencing revealed the splicing site of circHDAC1\_004. (C) HCC cDNA and gDNA samples were amplified with divergent and convergent primers of circHDAC1\_004, and the amplification products were detected by agarose gel electrophoresis. (D) qRT-PCR was performed to detect circHDAC1\_004 and HDAC1 mRNA in SK-Hep1 cells treated with or without RNase R digestion, and the results showed that circHDAC1\_004 was resistant to RNase R treatment. (E, F) Position of circHDAC1\_004 in HCC cells was identified by cytoplasmic separation (E) and the FISH (F) assay. The results revealed that circHDAC1\_004 was mainly located in the cytoplasm. Data are means  $\pm$  SDs. (NS, not significant; (\* $p$ <0.05; \*\* $p$ <0.01; \*\*\* $p$ <0.001). cDNA, Complementary DNA; gDNA, Genomic DNA.

metastatic tumor model. Subcutaneous tumor model experiments showed that the downregulation of circHDAC1\_004 inhibited tumor growth and its overexpression promoted tumor growth (Fig. 4A). In addition, immunohistochemical staining of subcutaneous tumors showed that Ki67, CD31, and vimentin were downregulated, and E-cadherin was upregulated in circHDAC1\_004 knockdown SK-Hep1 cells. Conversely, circHDAC1\_004 overexpression had the opposite result, further confirming that it promotes cell proliferation, HCC angiogenesis, and the EMT pathway in vivo (Fig. 4B). In the nude mouse lung metastases model, circHDAC1\_004 knockdown resulted in fewer and smaller lung metastases, whereas its

overexpression resulted in more and larger lung metastases (Fig. 4C). Collectively, these results suggest circHDAC1\_004 facilitated the proliferation, angiogenesis, and metastasis of HCC cells in vivo.

#### **circHDAC1\_004 was transferred from HCC cells to HUVECs through exosomes and promoted the angiogenesis of HCC**

Exosomes act as carriers to transport various bioactive substances between cells, and circRNAs can reportedly be transferred between cells by exosomes.<sup>13,14</sup> Exosomes were extracted from SK-Hep1 and YY8103 cells and detected by

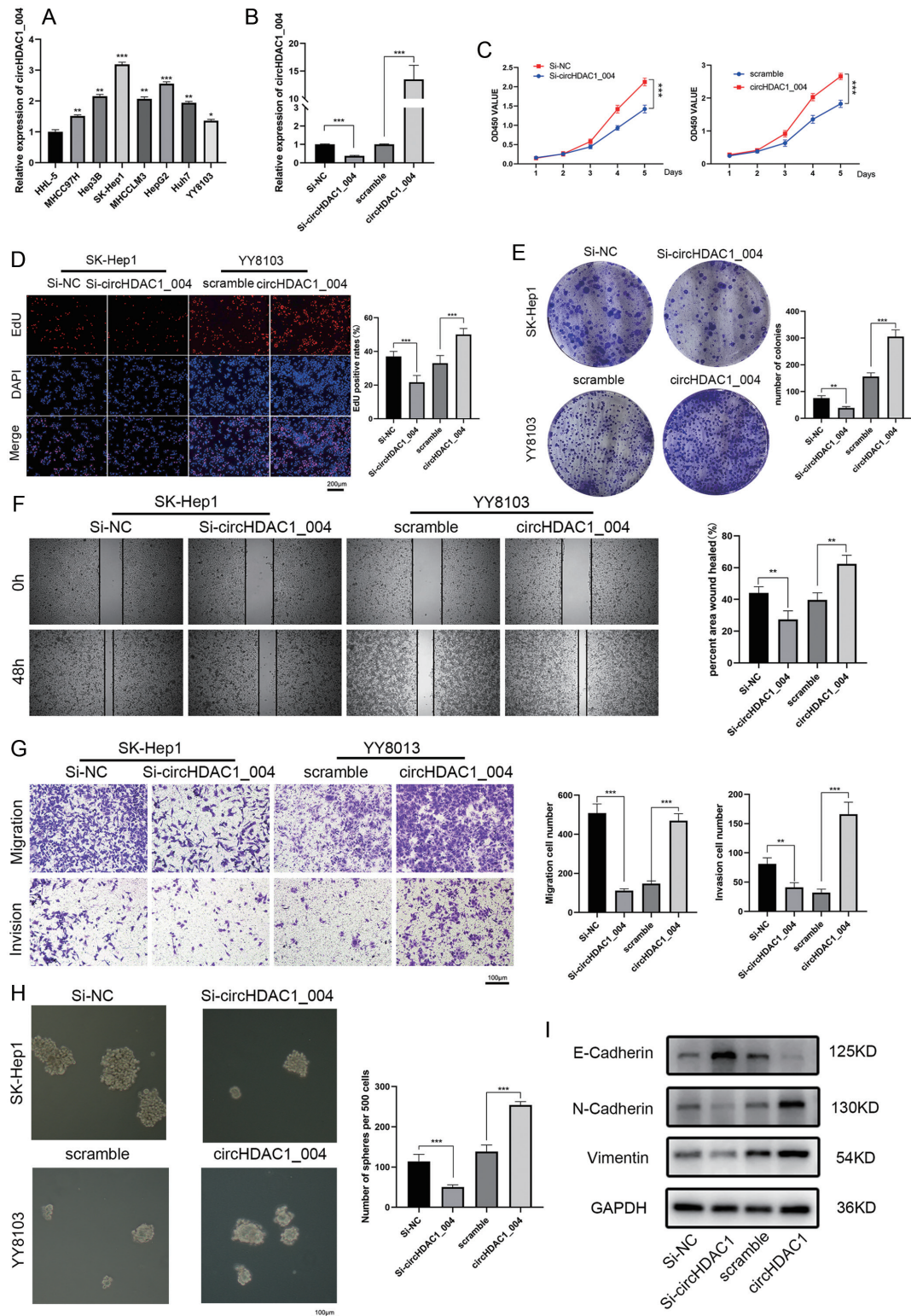


**Fig. 3. circHDAC1\_004 promoted HCC proliferation, migration, stemness, and EMT pathway.** (A) circHDAC1\_004 expression in HCC cell lines and HHL-5 (human embryonic hepatocytes). (B) The knockdown efficiency of circHDAC1\_004 in SK-Hep1 cells and its overexpression efficiency in YY8103 cells were detected by qRT-PCR. C-E. CCK-8 (C), EdU (D), and colony formation (E) assays were used to evaluate the proliferation ability of HCC cells with circ HDAC1\_004 knockdown or overexpression. (F-G) Migration and invasiveness of HCC cells were detected by wound healing (F) and Transwell assays (G). (H) The stemness of HCC cells with circ HDAC1\_004 knockdown or overexpression was verified by the sphere formation assay. (I) EMT-related proteins in HCC cells with circHDAC1\_004 knockdown or overexpression were detected by western blotting. Data are means  $\pm$  SD. (\* $p$ <0.05; \*\* $p$ <0.01; \*\*\* $p$ <0.001). CCK8, cell counting kit 8; EdU, 5-Ethynyl-20-deoxyuridine.



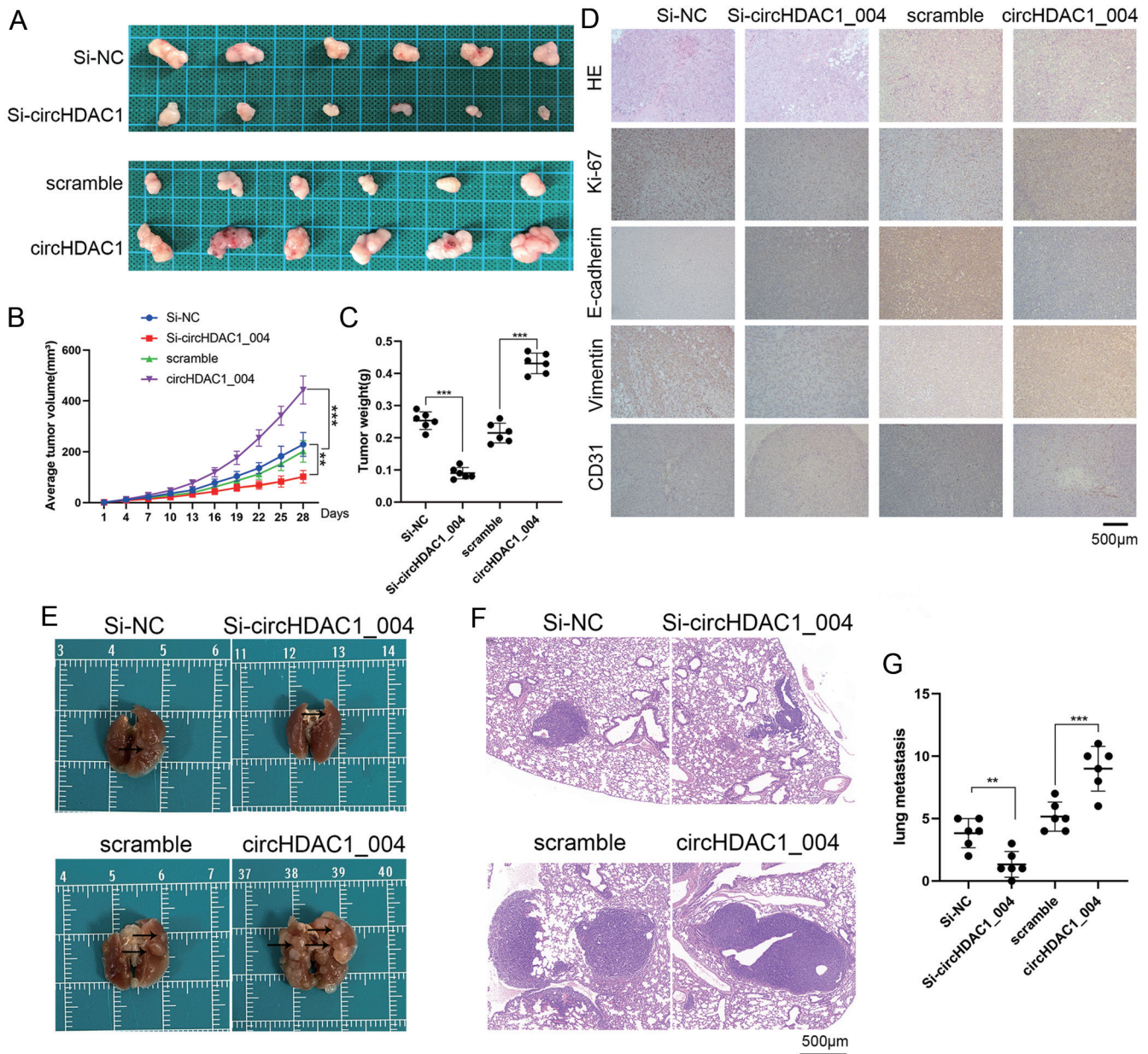


**Fig. 4. circHDAC1\_004 facilitated the proliferation and metastasis of HCC cells *in vivo*.** (A) Images of subcutaneous xenograft tumors derived from SK-Hep1 (Si-NC, Si-circHDAC1\_004) and YY8103 (scramble, circHDAC1\_004) cells. (B) Growth curve of the subcutaneous tumor volume. (C) Weight of the subcutaneous tumor. (D) HE, Ki67, E-cadherin, and vimentin staining of xenograft tumors. E-F Images (E) and hematoxylin and eosin staining (F) of lung metastases derived from SK-Hep1 and YY8103 cells. (G) Lung metastatic foci were counted. Data are means  $\pm$  SDs. (\* $p$ <0.05; \*\* $p$ <0.01; \*\*\* $p$ <0.001).

transmission electron microscopy (Fig. 5A). Nanoparticle tracking analysis showed that the peak size of exosomes was 50–150 nm (Fig. 5B). Meanwhile, the exosome markers CD81, CD9, and TSG101 were detected by western blotting (Fig. 5C). Agarose gel electrophoresis showed that circHDAC1\_004 could be detected in exosomes (Fig. 5D).

Tumor growth depends on angiogenesis,<sup>15</sup> for which exosome-derived circRNAs are important.<sup>13</sup> To investigate the function of exosomal circHDAC1\_004 in angiogenesis, we exposed HUVECs to exosomes isolated from SK-Hep1 and YY8103 cells with circHDAC1\_004 knockdown or overexpression. The uptake of PKH67-labeled exosomes by HU-

VECs was examined by confocal laser microscopy (Fig. 5E). PCR results showed that circHDAC1\_004 expression was downregulated in HUVECs co-cultured with circHDAC1\_004 knockdown exosomes and upregulated in HUVECs co-cultured with circHDAC1\_004 overexpression exosomes (Fig. 5F). Exosomes derived from circHDAC1\_004 knockdown SK-Hep1 cells inhibited the proliferation of HUVECs after 48 h of coculture, and those derived from circHDAC1\_004-overexpressing YY8103 cells promoted HUVEC proliferation (Supplementary Fig. 2A, B). The Transwell assay demonstrated that exosomes with low circHDAC1\_004 expression inhibited the ability of HUVECs to migrate compared to controls,



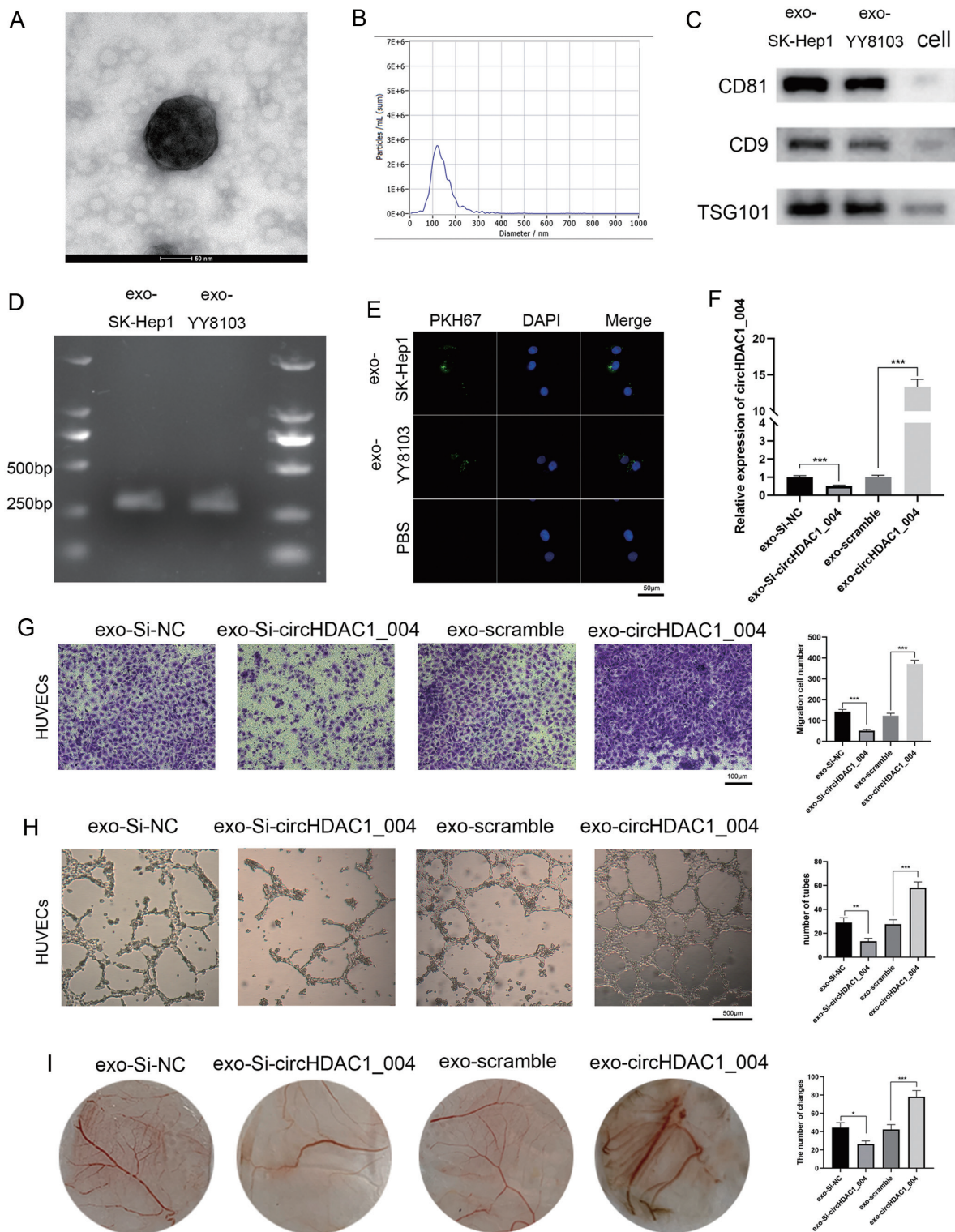


**Fig. 5. Exosomal circHDAC1\_004 promoted the proliferation, migration, and tube formation of HUVECs.** (A) Image of exosomes taken by transmission electron microscopy. (B) Nanoparticle tracking analysis (NTA) revealed that the peak size of exosomes was 50–150 nm. (C) Expression of exosome biomarkers was detected by western blotting. (D) circHDAC1\_004 in exosomes was amplified by PCR and then detected by agarose gel electrophoresis. (E) Laser confocal microscopy showed that the exosomes secreted by HCC cells were ingested by HUVECs. (F) qRT-PCR was performed to detect circHDAC1\_004 expression in HUVECs after coculture with circHDAC1\_004 knockdown or overexpression exosomes. (G) Migration of exosomes ingested by HUVECs was detected using the Transwell assay. (H) Tubule formation of exosomes ingested by HUVECs was verified using a tube formation assay. (I) Chick embryo chorioallantoic membrane assay showed that exosome circHDAC1\_004 promoted the angiogenesis of chick embryo chorioallantoic membrane. Data are means  $\pm$  SDs. (\* $p$ <0.05; \*\* $p$ <0.01; \*\*\* $p$ <0.001).

whereas exosomes with overexpressed circHDAC1\_004 promoted HUVEC migration (Fig. 5G). In addition, exosomes with circHDAC1\_004 knockdown inhibited the formation of HUVEC tubes, and those with circHDAC1\_004 overexpression had the opposite result (Fig. 5H). Furthermore, the chick embryo chorioallantoic membrane assay showed that exosomes with circHDAC1\_004 overexpression promoted angiogenesis in the membrane when compared with the control group, and exosomes with downregulated circHDAC1\_004 showed the opposite result (Fig. 5I). The results suggest that circHDAC1\_004 is transferred from HCC cells to HUVECs through exosomes and promotes HCC angiogenesis.

#### ***circHDAC1\_004 acts as a sponge of miR-361-3p***

Notably, circRNAs frequently function as miRNA sponges to regulate gene expression.<sup>16</sup> We predicted the downstream miRNAs of circHDAC1\_004 using the CircBank, Circinteractome, and Starbase databases. miR-361-3p and miR-194-5p have potential binding sites on circHDAC1\_004 (Fig. 6A). PCR results showed that miR-361-3p was downregulated in circHDAC1\_004-overexpressing YY8103 cells and upregulated in circHDAC1\_004 knockdown SK-Hep1 cells, whereas miR-194-5p expression did not differ between circHDAC1\_004 knockdown and overexpression groups (Fig. 6B, Supplementary Fig. 3A). Meanwhile, miR-361-3p expression was downregulated in HCC tissues and was negatively correlated with circHDAC1\_004 expression in 80 HCC tissues (Fig. 6C, D). miR-361-3p is an oncogene of HCC, and its expression was negatively correlated with the overall survival of HCC patients (Fig. 6E). Therefore, we speculated that it was a downstream miRNA of circHDAC1\_004. Furthermore, we designed a probe for circHDAC1\_004. A pull-down assay revealed that miR-361-3p could be pulled down (Fig. 6F) by the circHDAC1\_004 probe, and the RNA immunoprecipitation (RIP) assay indicated that both circHDAC1\_004 and miR-361-3p was enriched by the Ago2 antibody (Fig. 6G). To further explore the binding sites of circHDAC1\_004 and miR-361-3p, we designed WT and mutant circHDAC1\_004 vectors with luciferase according to the predicted binding sites (Fig. 6H). The luciferase activity of WT vectors was significantly reduced after coculturing with miR-361-3p mimics compared to mutant vectors (Fig. 6I). These results suggest that circHDAC1\_004 acted as a sponge for miR-361-3p.

#### ***NACC1 is a target gene of miR-361-3p***

Downstream target genes of miR-361-3p were predicted using Starbase, miRDIP, miRWalk, and miRDB, and the results of Venn diagram cross-linking suggested that miR-361-3p affects NACC1 expression (Fig. 7A). qRT-PCR results showed that NACC1 expression was upregulated in HCC tissues (Fig. 7B). Spearman correlation analysis indicated that NACC1 expression was negatively correlated with miR-361-3p (Fig. 7C) and positively correlated with circHDAC1\_004 (Fig. 7D). NACC1 expression was increased after miR-361-3p knockdown and decreased after miR-361-3p overexpression (Fig. 7E, F). Meanwhile, NACC1 expression decreased after circHDAC1\_004 knockdown and increased after circHDAC1\_004 overexpression (Fig. 7G, H). We performed a dual-luciferase reporter assay to determine the binding sites of miR-361-3p and NACC1-3' UTR. WT and mutant NACC1-3' UTR vectors with luciferase were designed according to the Targetscan database (Supplementary Fig. 4). The luciferase activity was significantly reduced in of miR-361-3p and NACC1 3' UTR-WT co-transfected cells but remained unchanged in miR-361-3p and NACC1 3' UTR-MUT cotransfected cells (Fig. 7I).

#### ***circHDAC1\_004 promoted HCC progression through the miR-361-3p/NACC1 axis***

To further explore the function of the circHDAC1\_004/miR-361-3p/NACC1 axis in HCC progression, miR-361-3p inhibitor or NACC1 overexpression vector were co-transfected in circHDAC1\_004 knockdown SK-Hep1 cells. Colony formation and 5-ethynyl-2'-deoxyuridine (EdU) assays showed that miR-361-3p knockdown and NACC1 overexpression restored the inhibitory effect of circHDAC1\_004 knockdown on HCC proliferation (Fig. 8A, Supplementary Fig. 5A). Transwell and wound healing assays revealed that both miR-361-3p inhibition and NACC1 overexpression effectively reversed the inhibitory effect of circHDAC1\_004 knockdown on HCC migration and invasion (Fig. 8B, Supplementary Fig. 5B). In addition, a stem cell sphere formation assay showed that the number of stem cell spheres reduced after circHDAC1\_004 knockdown but miR-361-3p knockdown or NACC1 overexpression reversed this phenomenon (Fig. 8C). In addition, Si-circHDAC1\_004 downregulated the EMT-related proteins N-cadherin and vimentin; upregulation of E-cadherin was also reversed by miR-361-3p inhibitor and NACC1 overexpression (Fig. 8D). The results suggested that circHDAC1\_004 increased NACC1 expression through competitive inhibition of inhibition of miR-361-3p, promoted the EMT pathway, and promoted HCC cell proliferation, migration, invasion, and stemness.

#### **Discussion**

Numerous studies have carried out in-depth analysis of the functions of HDAC1. Histone deacetylases (HDACs) catalyze the removal of acetyl groups from  $\epsilon$ -amino groups of lysine residues. Reversible acetylation of histone and nonhistone proteins by histone acetyltransferases (HATS) and histone deacetylases (HDACs) have key roles in transcriptional regulation in eukaryotic cells.<sup>17</sup> HDAC1 has novel functions in DNA replication and repair that contribute to chemotherapy resistance in cancer cells.<sup>18</sup> It has also been investigated in several HCC studies. It has been reported to inhibit FAM99A expression through histone H3 deacetylation transcription under hypoxic conditions, thus promoting HCC metastasis and EMT.<sup>19</sup> HDAC1 can also be used as a prognostic marker of HCC, which has significance for clinical treatment.<sup>20</sup> Further investigation of its mechanisms is needed because of the complex and diverse ways in which it regulates HCC. In the present study, we verified the expression and effect of 14 circRNAs derived from HDAC1 in HCC tissues.

Notably, circRNAs have received much attention for their potential diagnostic and therapeutic value; many studies have demonstrated their role in the diagnosis and treatment of HCC.<sup>21,22</sup> Huang *et al.*<sup>23</sup> showed that circMET drives immunosuppression and anti-PD1 treatment resistance in HCC via the miR-30-5p/SNAIL/DPP4 axis. Liu *et al.*<sup>24</sup> reported that the circRNA cIARS regulates iron death in HCC cells by interacting with the RNA-binding protein ALKBH530. Multiple signaling pathways, such as the Wnt,<sup>25,26</sup> YAP,<sup>27</sup> and PI3K/AKT/mTOR<sup>28</sup> signaling pathways, are involved in the development and progression of hepatocellular carcinoma. circRNAs are involved in various signaling pathways, such as the Wnt signaling pathway, to influence the development and progression of HCC.<sup>29</sup> Autophagy plays a pivotal role in tumorigenesis, metastasis, targeted therapy, and drug resistance in HCC.<sup>30</sup> Some studies have proved that circRNAs can trigger autophagy of HCC cells to affect disease progression. For example, Zhao *et al.*<sup>31</sup> demonstrated that circCBFB affects the progression of HCC by triggering cell autophagy through the miR-424-5p/ATG14 axis. To our knowledge, no

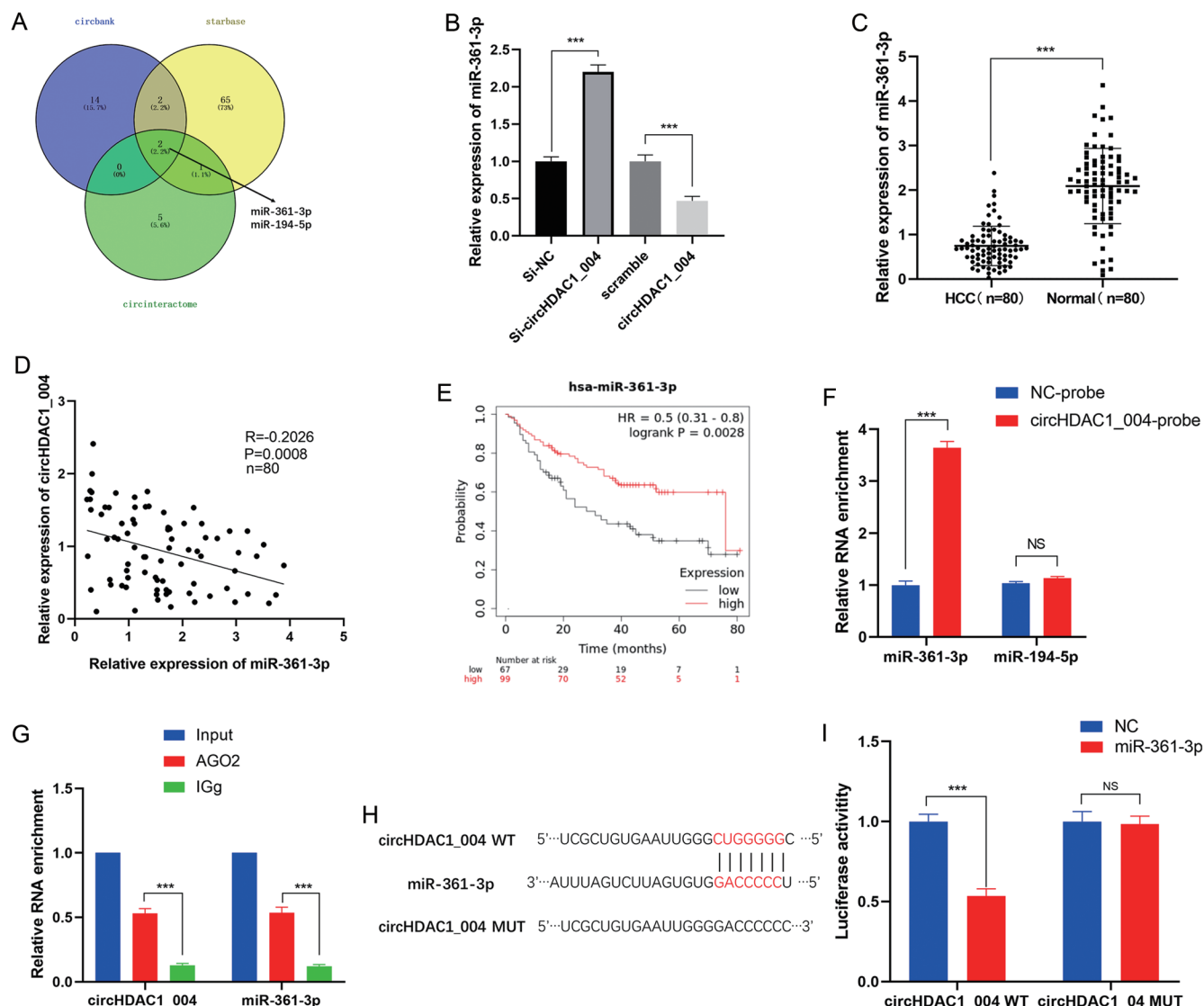


**Fig. 6. CircHDAC1\_004 acted as a sponge for miR-361-3p.** (A) Downstream miRNAs of circHDAC1\_004 were predicted from miRDB, miRDI, miRWalk, and Starbase databases. (B) miR-361-3p expression in Si-NC and Si-circHDAC1\_004 SK-Hep1 cells and in scramble and circHDAC1\_004 YH103 cells was detected by qRT-PCR. (C) miR-361-3p expression in HCC and paracancerous tissues was detected by qRT-PCR. (D) Spearman correlation analysis showed that circHDAC1\_004 expression was negatively correlated with the miR-361-3p expression. (E) The Starbase database showed that HCC patients with low miR-361-3p expression had a worse prognosis. (F) Pull-down assays showed that miR-361-3p was pulled down by the circHDAC1\_004 probe but miR-194-5p was not. (G) RIP assay showed that circHDAC1\_004 and miR-361-3p were enriched by the Ago2 antibody. (H) Wild-type (WT) and mutant plasmids (MUT) of circ HDAC1\_004 were designed according to the Starbase database. (I) Luciferase activity in HEK-293T cells co-transfected with WT or MUT circHDAC1\_004 sequences and miR-361-3p mimics or controls. Data are means  $\pm$  SDs. (NS, not significant; \* $p$ <0.05; \*\* $p$ <0.01; \*\*\* $p$ <0.001). RIP, RNA binding protein Immunoprecipitation.

studies have been conducted on circRNAs transcribed by HDAC1 thus far, and we explored whether these circRNAs have biological functions in HCC. In this study, we found that circHDAC1\_004 expression was upregulated in HCC tissues and negatively correlated with HCC prognosis. *In vitro* experiments showed that circHDAC1\_004 knockdown inhibited cell proliferation, migration, stemness, and the EMT pathway, which were enhanced after circHDAC1\_004 overexpression. *In vivo* experiments further demonstrated that circHDAC1\_004 promoted the proliferation and metastasis of HCC cells. Thus, circHDAC1\_004 had a carcinogenic role in HCC and was involved in the occurrence and progression of HCC.

Angiogenesis is considered a hallmark of cancer, and significant vascular abnormalities are an important cause of

liver injury leading to HCC<sup>11</sup>. Some studies have explored the effects of circRNAs in exosomes on HCC angiogenesis.<sup>32</sup> Huang *et al.*<sup>13</sup> found that exosome-derived circRNA-100338 promoted HCC angiogenesis by binding with RNA-binding proteins. We found that circHDAC1\_004 were secreted into the HCC tumor microenvironment by exosomes. Coculture of HUVECs with exosomes with circHDAC1\_004 knockdown or overexpression revealed that exosomal circHDAC1\_004 promoted tube formation, proliferation, and migration of HUVECs. These results indicate that circHDAC1\_004 upregulation in HCC cells promoted HCC angiogenesis through exosomes.

Next, we discuss the mechanism of circHDAC1\_004 in HCC. Many studies have shown that the circRNA-miRNA-



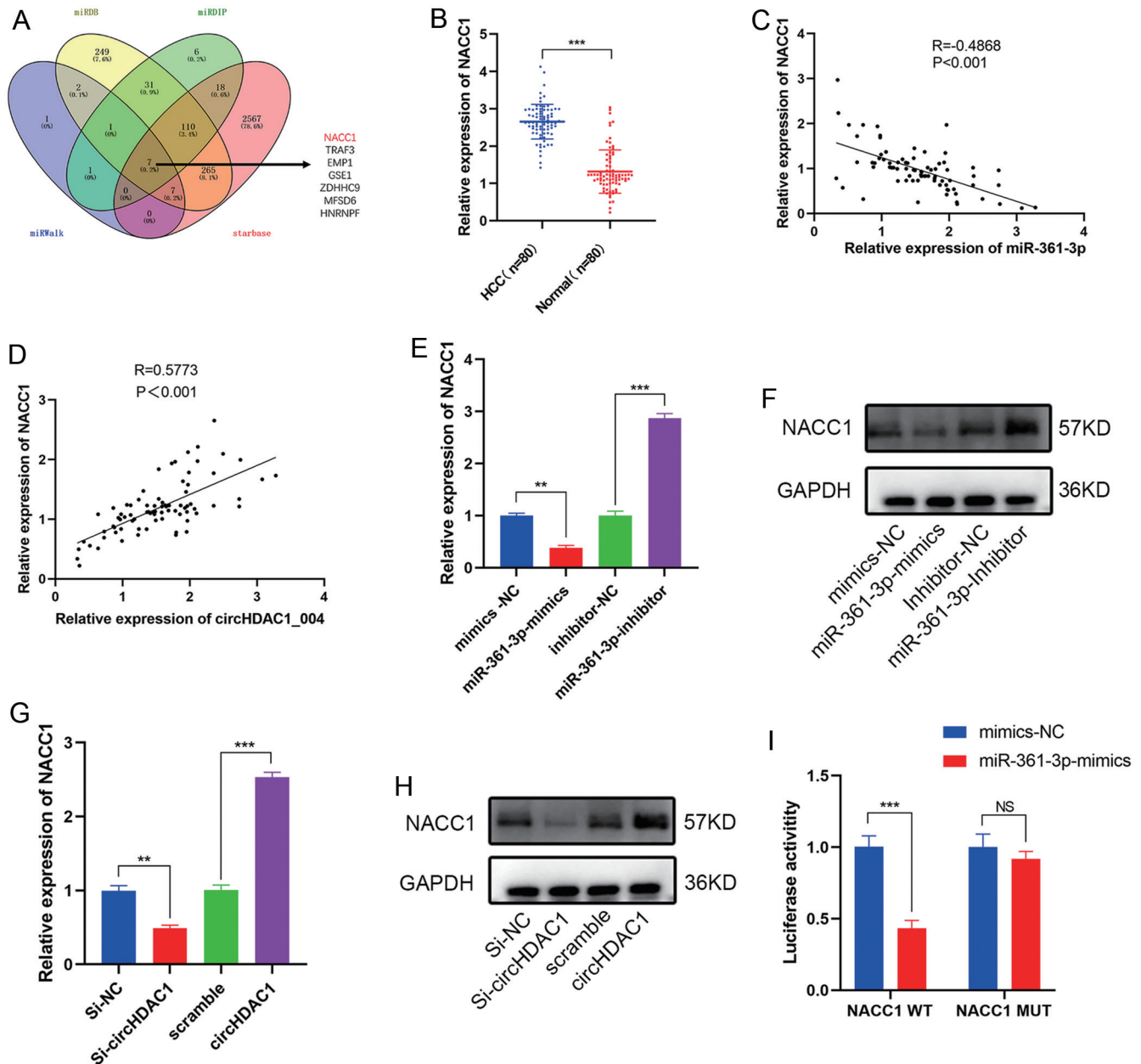


**Fig. 7. NACC1 was one target gene of miR-361-3p.** (A) The database predicted NACC1 as a downstream target protein of miR-361-3p. (B) NACC1 was highly expressed in HCC tissues. C-(D) Spearman correlation was used to analyze the correlation between NACC1 and miR-361-3p (C) or circHDAC1\_004 (D). (E, F) Relative mRNA and protein levels of NACC1 after knockdown or overexpression of miR-361-3p in HCC cells were detected by qRT-PCR (E) and western blotting (F). (G, H) qRT-PCR (G) and western blotting (H) were performed to detect relative mRNA and protein levels of NACC1 in HCC cells with circHDAC1\_004 knockdown or overexpression, respectively. (I) Luciferase activity was measured in HEK-293T cells cotransfected with NACC1-WT or NACC1-MUT luciferase plasmid and with miR-361-3p mimic or control. Data are means  $\pm$  SDs. (NS, not significant; (\* $p < 0.05$ ; \*\* $p < 0.01$ ; \*\*\* $p < 0.001$ ).

mRNA interaction mechanism significantly affects the occurrence and development of different cancers, including HCC.<sup>33</sup> Zhang *et al.*<sup>34</sup> found that circRNA103809 promoted the malignant progression of HCC through the miR-377-3p/FGFR1/ERK axis. The nucleoplasmic separation and FISH assays revealed that circHDAC1\_004 is mainly located in the cytoplasm. We identified miR-361-3p to be a downstream miRNA of circHDAC1\_004 in HCC and further explored the downstream target genes of circHDAC1\_004/miR-361-3p. We also found that NACC1 expression was influenced by

miR-361-3p. It was promoted by circHDAC1\_004 and inhibited by miR-361-3p. NACC1 has a cancer-promoting role in various malignant tumors and has potential diagnostic and therapeutic value.<sup>35,36</sup> Yin *et al.*<sup>37</sup> identified NACC1 as an oncogene in HCC. Rescue studies have reported that both miR-361-3p inhibitor and NACC1 overexpression could rescue the inhibition of circHDAC1\_004 knockdown on cell proliferation, migration, invasion, cell stemness, and the EMT pathway in HCC. All the above data suggest that the circHDAC1\_004/miR-361-3p/NACC1 axis plays a key role



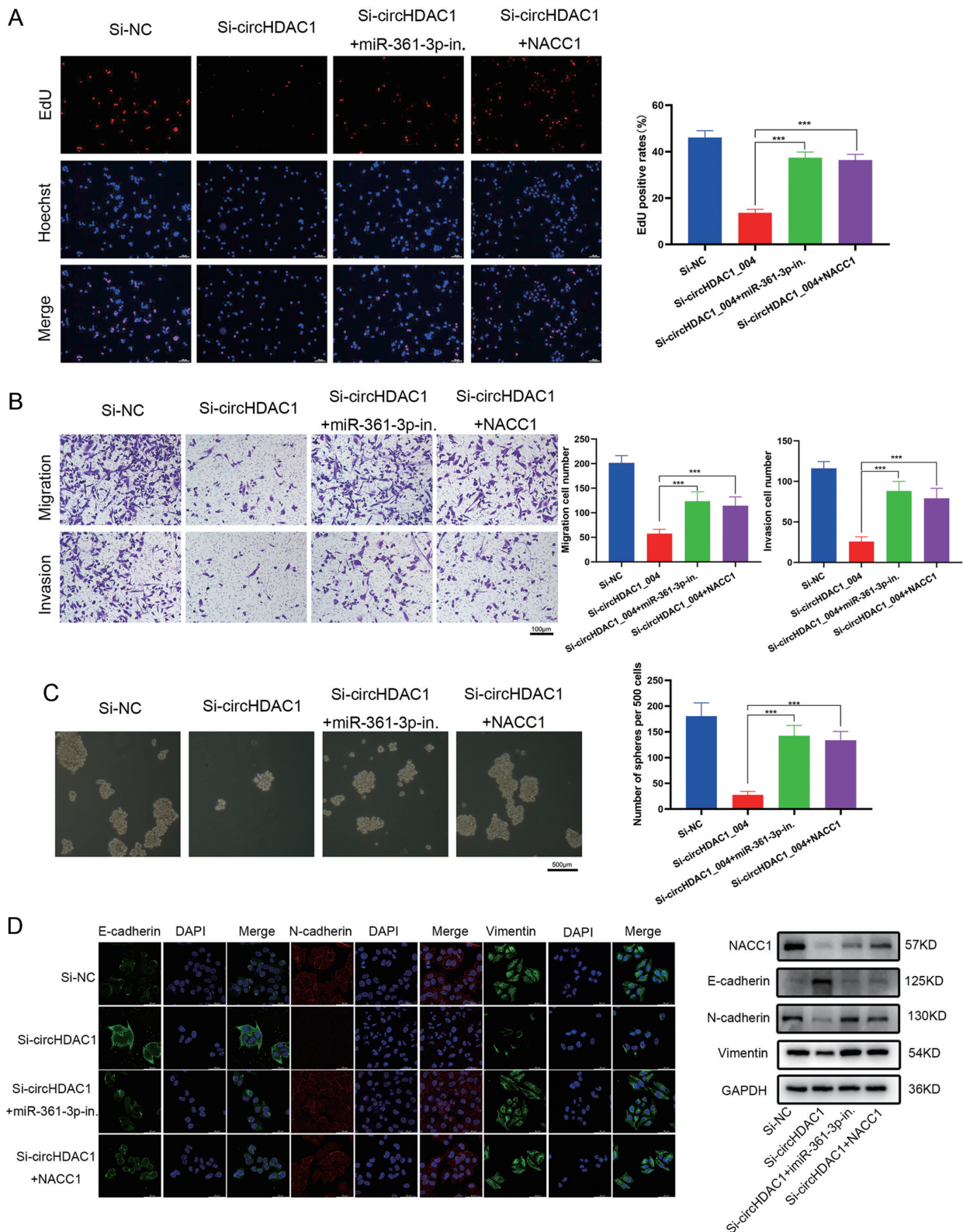


**Fig. 8. Rescue experiments confirmed the function of the circHDAC1\_004/miR-361-3p/NACC1 axis in HCC.** (A) EdU assays were used to examine the proliferative ability of different groups. (B) Transwell assays were used to verify the migration and invasion ability of HCC cells in different treatment groups. (C) Stemness of HCC cells in different treatment groups was detected using the sphere formation assay. (D) Expression of EMT-related proteins in different groups of HCC cells was detected by immunofluorescence (left) and western blotting (right). (miR-361-3p-in, miR-361-3p inhibitor). Data are means  $\pm$  SDs. (\* $p$ <0.05; \*\* $p$ <0.01; \*\*\* $p$ <0.001).

in HCC.

Although there are many methods for the diagnosis and treatment of HCC, their clinical efficacy is not ideal, and we therefore urgently need new avenues to improve the existing means of diagnosis and treatment. Exosomes are rich biomarkers for disease diagnosis and prognosis. Recently, exosomes have been widely used in the diagnosis of cancer.<sup>38</sup> At present, various molecular targeted drugs have been applied in the clinical treatment of HCC, such as sorafenib and Lenvatinib. However, not all HCC patients have good results with these drugs.<sup>39</sup> Considering the important role of circHDAC1\_004 in the occurrence and progression of HCC, we believe that circHDAC1\_004 can be used as a diagnostic marker for HCC. In addition, circHDAC1\_004 may also be a new target for HCC.

## Conclusion

In conclusion, we confirmed the significant role of circHDAC1\_004 in the development of HCC. circHDAC1\_004 expression was upregulated in HCC cells, wherein it promoted cell proliferation, migration, stemness, and the EMT pathway. In addition, circHDAC1\_004 was secreted out of HCC cells by exosomes to promote HCC angiogenesis. circHDAC1\_004 promoted NACC1 expression by competitively binding miR-361-3p. To our knowledge, this study is the first to investigate the role of circHDAC1\_004 in HCC and the specific mechanism by which circHDAC1\_004 promotes HCC, which may help provide a novel treatment strategy for HCC.

## Acknowledgments

We thank Medjaden for providing us with writing assistance.

## Funding

The work was supported by the National Natural Science Foundation of China (grant number 81871260); The training programme of "Double hundred" young and middle-aged medical and health talents in Wuxi ((grant number BJ020034); Health Research Projects of Wuxi Health Committee ((grant number M202106).

## Conflict of interest

The authors have no conflict of interests related to this publication.

## Author contributions

Study concept and design (LK, WD, YZ), acquisition of data (BX, WJ, YF, JyW), analysis and interpretation of data (JW, DZ, CX, LL), drafting of the manuscript (BX, WJ). All authors have made a significant contribution to this study and have approved the final manuscript.

## Ethical statement

Ethical approval was obtained from the Ethics Committee of the First Affiliated Hospital of Nanjing Medical University (2022-SRFA-221), and written informed consent was obtained from each patient. All animal experiments in this study were approved by the Institutional Animal Care and Use Committee of the First Affiliated Hospital of Nanjing Medical University (IACUC-2109022). Informed consent was obtained from all individual participants included in the study.

## Data sharing statement

The qPCR, western blot, and other data used to support the findings of this study are included within the article.

## References

- [1] Marquardt JU, Andersen JB, Thorgeirsson SS. Functional and genetic deconstruction of the cellular origin in liver cancer. *Nat Rev Cancer* 2015;15(11):653–667. doi:10.1038/nrc4017, PMID:26493646.
- [2] Jemal A, Bray F, Center MM, Ferlay J, Ward E, Forman D. Global cancer statistics. *CA Cancer J Clin* 2011;61(2):69–90. doi:10.3322/caac.20107, PMID:21296855.
- [3] Forner A, Reig M, Bruix J. Hepatocellular carcinoma. *Lancet* 2018;391(10127):1301–1314. doi:10.1016/S0140-6736(18)30010-2, PMID:29307467.
- [4] Vicens Q, Westhof E. Biogenesis of Circular RNAs. *Cell* 2014;159(1):13–14. doi:10.1016/j.cell.2014.09.005, PMID:25259915.
- [5] Ebert MS, Sharp PA. MicroRNA sponges: progress and possibilities. *RNA* 2010;16(11):2043–2050. doi:10.1261/rna.2414110, PMID:20855538.
- [6] Kato T, Shimono Y, Hasegawa M, Jijiwa M, Enomoto A, Asai N, *et al*. Characterization of the HDAC1 complex that regulates the sensitivity of cancer cells to oxidative stress. *Cancer Res* 2009;69(8):3597–3604. doi:10.1158/0008-5472.CAN-08-4368, PMID:19351825.
- [7] Lager G, Doetzelhofer A, Schuettengruber B, Haidweger E, Simboeck E, Tischler J, *et al*. The tumor suppressor p53 and histone deacetylase 1 are antagonistic regulators of the cyclin-dependent kinase inhibitor p21/WAF1/CIP1 gene. *Mol Cell Biol* 2003;23(8):2669–2679. doi:10.1128/MCB.23.8.2669-2679.2003, PMID:12665570.
- [8] Juan LJ, Shia WJ, Chen MH, Yang WM, Seto E, Lin YS, *et al*. Histone deacetylases specifically down-regulate p53-dependent gene activation. *J Biol Chem* 2000;275(27):20436–20443. doi:10.1074/jbc.M00020200, PMID:10777477.
- [9] Oh YM, Kwon YE, Kim JM, Bae SJ, Lee BK, Yoo SJ, *et al*. Chfr is linked to tumour metastasis through the downregulation of HDAC1. *Nat Cell Biol* 2009;11(3):295–302. doi:10.1038/ncb1837, PMID:19182791.
- [10] Melo SA, Sugimoto H, O'Connell JT, Kato N, Villanueva A, Vidal A, *et al*. Cancer exosomes perform cell-independent microRNA biogenesis and promote tumorigenesis. *Cancer Cell* 2014;26(5):707–721. doi:10.1016/j.ccr.2014.09.005, PMID:25446899.
- [11] Roma-Rodrigues C, Raposo LR, Cabral R, Paradinha F, Baptista PV, Fernandes AR. Tumor Microenvironment Modulation via Gold Nanoparticles Targeting Malicious Exosomes: Implications for Cancer Diagnostics and Therapy. *Int J Mol Sci* 2017;18(1):162. doi:10.3390/ijms18010162, PMID:28098821.
- [12] Pan G, Liu Y, Shang L, Zhou F, Yang S. EMT-associated microRNAs and their roles in cancer stemness and drug resistance. *Cancer Commun (Lond)* 2021;41(3):199–217. doi:10.1002/cac2.12138, PMID:33506604.
- [13] Huang XY, Huang ZL, Huang J, Xu B, Huang XY, Xu YH, *et al*. Exosomal circRNA-100338 promotes hepatocellular carcinoma metastasis via enhancing invasiveness and angiogenesis. *J Exp Clin Cancer Res* 2020;39(1):20. doi:10.1186/s13046-020-1529-9, PMID:31973767.
- [14] Li Y, Zheng Q, Bao C, Li S, Guo W, Zhao J, *et al*. Circular RNA is enriched and stable in exosomes: a promising biomarker for cancer diagnosis. *Cell Res* 2015;25(8):981–984. doi:10.1038/cr.2015.82, PMID:26138677.
- [15] Plate KH, Scholz A, Dumont DJ. Tumor angiogenesis and anti-angiogenic therapy in malignant gliomas revisited. *Acta Neuropathol* 2012;124(6):763–775. doi:10.1007/s00401-012-1066-5, PMID:23143192.
- [16] Cao P, Jin Q, Feng L, Li H, Qin G, Zhou G. Emerging roles and potential clinical applications of noncoding RNAs in hepatocellular carcinoma. *Semin Cancer Biol* 2021;75:136–152. doi:10.1016/j.semcancer.2020.09.003, PMID:32931952.
- [17] Kim MY, Yan B, Huang S, Qiu Y. Regulating the Regulators: The Role of Histone Deacetylase 1 (HDAC1) in Erythropoiesis. *Int J Mol Sci* 2020;21(22):8460. doi:10.3390/ijms21228460, PMID:33187090.
- [18] Bhaskara S. Histone deacetylases 1 and 2 regulate DNA replication and DNA repair: potential targets for genome stability-mechanism-based therapeutics for a subset of cancers. *Cell Cycle* 2015;14(12):1779–1785. doi:10.1080/15384101.2015.1042634, PMID:25942572.
- [19] Zhao B, Ke K, Wang Y, Wang F, Shi Y, Zheng X, *et al*. HIF-1α and HDAC1 mediated regulation of FAM99A-miR92a signaling contributes to hypoxia induced HCC metastasis. *Signal Transduct Target Ther* 2020;5(1):118. doi:10.1038/s41392-020-00223-6, PMID:32636357.
- [20] Yang Z, Zhou L, Wu LM, Xie HY, Zhang F, Zheng SS. Combination of polymorphisms within the HDAC1 and HDAC3 gene predict tumor recurrence in hepatocellular carcinoma patients that have undergone transplant therapy. *Clin Chem Lab Med* 2010;48(12):1785–1791. doi:10.1515/CCLM.2010.353, PMID:20731616.
- [21] Wei L, Wang X, Lv L, Liu J, Xing H, Song Y, *et al*. The emerging role of microRNAs and long noncoding RNAs in drug resistance of hepatocellular carcinoma. *Mol Cancer* 2019;18(1):147. doi:10.1186/s12943-019-1086-z, PMID:31651347.
- [22] Wong CM, Tsang FH, Ng IO. Non-coding RNAs in hepatocellular carcinoma: molecular functions and pathological implications. *Nat Rev Gastroenterol Hepatol* 2018;15(3):137–151. doi:10.1038/nrgastro.2017.169, PMID:29317776.
- [23] Huang XY, Zhang PF, Wei CY, Peng R, Lu JC, Gao C, *et al*. Circular RNA circMET drives immunosuppression and anti-PD1 therapy resistance in hepatocellular carcinoma via the miR-30-5p/snail/DPP4 axis. *Mol Cancer*

Xu B. *et al*: circHDAC1\_004 promotes HCC progression.

- 2020;19(1):92. doi:10.1186/s12943-020-01213-6, PMID:32430013.
- [24] Liu Z, Wang Q, Wang X, Xu Z, Wei X, Li J. Circular RNA ciARS regulates ferroptosis in HCC cells through interacting with RNA binding protein ALKBH5. *Cell Death Discov* 2020;6:72. doi:10.1038/s41420-020-00306-x, PMID:32802409.
- [25] Zhang J, Lai W, Li Q, Yu Y, Jin J, Guo W, *et al*. A novel oncolytic adenovirus targeting Wnt signaling effectively inhibits cancer-stem like cell growth via metastasis, apoptosis and autophagy in HCC models. *Biochem Biophys Res Commun* 2017;491(2):469–477. doi:10.1016/j.bbrc.2017.07.041, PMID:28698142.
- [26] Wang Y, Huang P, Hu Y, Guo K, Jia X, Huang B, *et al*. An oncolytic adenovirus delivering TSLC1 inhibits Wnt signaling pathway and tumor growth in SMMC-7721 xenograft mice model. *Acta Biochim Biophys Sin (Shanghai)* 2021;53(6):766–774. doi:10.1093/abbs/gmab048, PMID:33928346.
- [27] Zhang X, Li Y, Ma Y, Yang L, Wang T, Meng X, *et al*. Yes-associated protein (YAP) binds to HIF-1 $\alpha$  and sustains HIF-1 $\alpha$  protein stability to promote hepatocellular carcinoma cell glycolysis under hypoxic stress. *J Exp Clin Cancer Res* 2018;37(1):216. doi:10.1186/s13046-018-0892-2, PMID:30180863.
- [28] Wu Y, Zhang Y, Qin X, Geng H, Zuo D, Zhao Q. PI3K/AKT/mTOR pathway-related long non-coding RNAs: roles and mechanisms in hepatocellular carcinoma. *Pharmacol Res* 2020;160:105195. doi:10.1016/j.phrs.2020.105195, PMID:32916254.
- [29] Huang G, Liang M, Liu H, Huang J, Li P, Wang C, *et al*. CircRNA hsa\_circRNA\_104348 promotes hepatocellular carcinoma progression through modulating miR-187-3p/RTKN2 axis and activating Wnt/ $\beta$ -catenin pathway. *Cell Death Dis* 2020;11(12):1065. doi:10.1038/s41419-020-03276-1, PMID:33311442.
- [30] Huang F, Wang BR, Wang YG. Role of autophagy in tumorigenesis, metastasis, targeted therapy and drug resistance of hepatocellular carcinoma. *World J Gastroenterol* 2018;24(41):4643–4651. doi:10.3748/wjg.v24.i41.4643, PMID:30416312.
- [31] Zhao Z, He J, Feng C. CircCBFB is a mediator of hepatocellular carcinoma cell autophagy and proliferation through miR-424-5p/ATG14 axis. *Immunol Res* 2022;70(3):341–353. doi:10.1007/s12026-021-09255-8, PMID:35066780.
- [32] Morse MA, Sun W, Kim R, He AR, Abada PB, Mynderse M, *et al*. The Role of Angiogenesis in Hepatocellular Carcinoma. *Clin Cancer Res* 2019;25(3):912–920. doi:10.1158/1078-0432.CCR-18-1254, PMID:30274981.
- [33] Hu J, Li P, Song Y, Ge YX, Meng XM, Huang C, *et al*. Progress and prospects of circular RNAs in Hepatocellular carcinoma: Novel insights into their function. *J Cell Physiol* 2018;233(6):4408–4422. doi:10.1002/jcp.26154, PMID:28833094.
- [34] Zhan W, Liao X, Chen Z, Li L, Tian T, Yu L, *et al*. Circular RNA hsa\_circRNA\_103809 promoted hepatocellular carcinoma development by regulating miR-377-3p/FGFR1/ERK axis. *J Cell Physiol* 2020;235(2):1733–1745. doi:10.1002/jcp.29092, PMID:31317555.
- [35] Yang T, Shen P, Chen Q, Wu P, Yuan H, Ge W, *et al*. FUS-induced circRHOB-TB3 facilitates cell proliferation via miR-600/NACC1 mediated autophagy response in pancreatic ductal adenocarcinoma. *J Exp Clin Cancer Res* 2021;40(1):261. doi:10.1186/s13046-021-02063-w, PMID:34416910.
- [36] Cao Z, Chen H, Mei X, Li X. Silencing of NACC1 inhibits the proliferation, migration and invasion of nasopharyngeal carcinoma cells via regulating the AKT/mTOR signaling pathway. *Oncol Lett* 2021;22(6):828. doi:10.3892/ol.2021.13088, PMID:34691255.
- [37] Yin L, Sun T, Liu R. NACC-1 regulates hepatocellular carcinoma cell malignancy and is targeted by miR-760. *Acta Biochim Biophys Sin (Shanghai)* 2020;52(3):302–309. doi:10.1093/abbs/gmz167, PMID:32091103.
- [38] Zhang Y, Bi J, Huang J, Tang Y, Du S, Li P. Exosome: A Review of Its Classification, Isolation Techniques, Storage, Diagnostic and Targeted Therapy Applications. *Int J Nanomedicine* 2020;15:6917–6934. doi:10.2147/IJN.S264498, PMID:33061359.
- [39] Couri T, Pillai A. Goals and targets for personalized therapy for HCC. *Hepatol Int* 2019;13(2):125–137. doi:10.1007/s12072-018-9919-1, PMID:30600478.